JOURNAL OF GUIDANCE, CONTROL, AND DYNAMICS
Vol. 19, No. 6, November–December 1996

Mixed Linear-Quadratic/Eigenstructure Strategy for Design of Stability Augmentation Systems

Giovanni Mengali*
University of Pisa, Pisa 56126, Italy

The problem of determining an optimal output-feedback controller that forces the aircraft dynamics to evolve as an ideal model with prescribed eigenvalues and eigenvectors is addressed. A mixed linear-quadratic/eigenstructure strategy is used, where the matrix gain is chosen by minimizing a standard quadratic performance criterion. This allows one to 1) keep under control the maximum value of the input demand and 2) take into account flying-quality requirements by imposing suitable constraints on the system eigenstructure. It is believed that this optimization procedure provides significant improvements to a standard eigenstructure strategy and that it is well suited in the design of aircraft stability augmentation systems. A discussion of three case studies demonstrates the effectiveness of this procedure by comparing the corresponding results with others given in the literature.

Introduction

THE design of aircraft control systems deals with a variety of different engineering problems, for instance, longitudinal and lateral stability enhancement, ride-quality improvement, elastic-mode suppression, and flutter prevention. A broad class of these problems can be mathematically modeled by employing suitable control laws that force the aircraft to behave like an ideal linear model. This approach is particularly convenient for the design of stability augmentation systems, which are control methods providing the free-response modes of the aircraft with suitable damping and natural frequencies. They modify isolated stability features of the airframe alone in such a way that the cockpit controls are unaffected[1] and aircraft flying-quality requirements are met. Basically, it should be guaranteed that poles and zeros of the aircraft model lie within prescribed regions of the complex plane.[2]

For these reasons the eigenstructure assignment has found a remarkable interest, especially after Moore[3] pointed out the power of full-state feedback in completely specifying the closed-loop eigenvalues and partially assigning the corresponding eigenvectors. Since then, a number of papers have been written on eigenstructure assignment, generalizing Moore's results to output-feedback systems[4] and constrained output feedback.[5,6] An excellent review of these topics is given by Andry et al.[5] Applications of eigenstructure assignment to flight control systems also are given elsewhere.[7–10]

The main drawback of the eigenstructure assignment approach is that it is difficult to constrain the maximum values of rotation angles and deflection velocity of the control surfaces. From this point of view, a preferable method is to employ a standard linear quadratic (LQ) design, where the quadratic performance index (PI) directly allows one to limit the control demand. In this case, however, it is hard to tailor eigenvalues and eigenvectors of the controlled system and, indeed, many efforts have been made to try to combine the two techniques.

Early contributions in this area were made by Harvey and Stein,[11] who indicated how to select control weights to obtain desired pole configurations in the limit as the weights tend to zero. More recently, the problem of designing LQ controllers with desired pole locations has received a new impetus, and different pole constraint regions have been studied.[12–15] The results are basically obtained through a transformation that maps the constraint region into the left half-plane, and the feedback gains then are obtained by using a Lyapunov equation. Following another point of view, Slater and Zhang[16] proposed a controller design strategy for eigenstructure assignment by imposing that the desired closed-loop eigenvectors be a linear combination of a subset of open-loop eigenvectors. This technique has been applied successfully to problems related to the active vibration control of flexible structures.

Our approach here is completely different from all that have been previously recalled. Our contribution is to extend the preceding results by formulating a consistent method that allows one to constrain eigenvalues as well as eigenvectors and, at the same time, to take into account the problem of controlling the maximum input demand of the deflection surfaces. In this way, the classic drawback related to eigenstructure design is overcome. In doing so, the standard approach employing Lyapunov equations for synthesizing feedback gains has not been recovered. This fact, however, should not be considered as a serious obstacle degrading the computational performance of the proposed algorithm. Indeed, the key observation is exploited that knowledge of the relation between output gain matrix K and state matrix of the controlled system allows one to evaluate a standard quadratic PI in closed form. This line of reasoning leads to an efficient numerical optimization procedure in which the constraints over the eigenvalues and eigenvectors are easily taken into account by means of a mixed LQ/eigenstructure approach.

System Model and Control Law

The aircraft dynamics are described by the following linear time-invariant system:

$$\dot{x} = Ax + Bu; \qquad x(0) = x_o \tag{1}$$

$$y = Cx \tag{2}$$

and by the output-feedback-control law

$$u = -Ky \tag{3}$$

Here, $x \in R^n$ denotes the state of the system, $u \in R^m$ indicates the input (or control) variable, and $y \in R^r$ is the output variable. All x, u, and y are functions of time t. In the following, we assume that the system is controllable and observable and that the matrices B and C are of full rank.

The closed-loop system dynamics are given by

$$\dot{x} = A_c x; \qquad x(0) = x_o \tag{4}$$

with

$$A_c = A - BKC \tag{5}$$

In the classic LQ design, the following PI is minimized:

$$J = E\left\{\int_0^\infty (x^T Q x + u^T R u)\,dt\right\} \tag{6}$$

where $E\{\cdot\}$ is the expectation operator and $Q \geq 0$, $R > 0$ are weighting matrices assigned by the user. The presence of $E\{\cdot\}$ in

Received May 11, 1995; revision received May 28, 1996; accepted for publication June 6, 1996.

*Assistant Professor, Dipartimento di Ingegneria Aerospaziale, Via Diotisalvi, 2.

Eq. (6) avoids the undesirable dependence of PI on the initial state $x(0)$.[17]

The major drawback with the LQ approach is that the designer cannot choose the location of the eigenvalues or shape the eigenvectors of the closed-loop system, so that this technique is impractical in the synthesis of aircraft stability augmentation systems. Hence, the necessity arises of minimizing the PI while imposing some constraints on the eigenvalues and eigenvectors of A_c. To this end, assuming that all eigenvalues of A_c are distinct, we put

$$A_c = M \Lambda M^{-1} \tag{7}$$

where M is the modal matrix and Λ is the block-diagonal matrix containing the eigenvalues of A_c. The free response of the controlled system is given by

$$x = M e^{\Lambda t} M^{-1} x_o \tag{8}$$

Substituting Eqs. (2), (3), and (8) into Eq. (6) yields

$$J = E\left\{ \int_0^\infty \left[\xi_o^T \Phi^T(t) T \Phi(t) \xi_o \right] \mathrm{d}t \right\} \tag{9}$$

where

$$\xi_o \equiv M^{-1} x_o \tag{10}$$

$$T \equiv M^T (Q + C^T K^T R K C) M \tag{11}$$

$$\Phi(t) \equiv e^{\Lambda t} \tag{12}$$

Note that, as a consequence of Eq. (9), the PI can be transformed into

$$J = \mathrm{tr}(ZX) \tag{13}$$

where $\mathrm{tr}(\cdot)$ is the trace operator and

$$X \equiv E\left\{ \xi_o \xi_o^T \right\} = M^{-1} E\left\{ x_o x_o^T \right\} (M^{-1})^T \tag{14}$$

$$Z \equiv \int_0^\infty [\Phi^T(t) T \Phi(t)] \, \mathrm{d}t \tag{15}$$

Note that X [and also J, as a consequence of Eq. (13)], is a function of the initial autocorrelation of the state, $E\{x_o x_o^T\}$. It is customary[17] to select $E\{x_o x_o^T\} = I$, which reflects an initial state uniformly distributed on a unit sphere.

To compute PI for a given A_c, the following is needed: 1) fix the correspondence law between the eigenstructure of A_c and the gain matrix K; and 2) perform the integration appearing in the Z matrix in Eq. (15). Hereafter, we show that this integral can be given in closed form, which makes the computation of PI quite efficient.

PI Evaluation

According to Srinathkumar,[4] in the eigenstructure assignment problem it is possible to assign $\max(m, r)$ number of eigenvalues and $\min(m, r)$ number of components of the corresponding right eigenvectors. With this choice, it is possible to evaluate a K matrix so that the corresponding A_c matrix has the desired eigenstructure. Without loss of generality, we assume $r > m$. Following Moore's guidelines,[2] we consider a linear system whose unknowns are the closed-loop eigenvector v_i, corresponding to the eigenvalue λ_i, and the auxiliary vector u_i such that

$$\begin{bmatrix} \lambda_i I - A & B \\ D & 0 \end{bmatrix} \begin{bmatrix} v_i \\ u_i \end{bmatrix} = \begin{bmatrix} 0 \\ v_i^d \end{bmatrix} \tag{16}$$

where $v_i^d \in R^m$ is formed by the m components (assignable by the user) of v_i. D is a matrix, with entries 0 or 1, that allows one to establish which components of v_i assume the values specified by v_i^d. For example, suppose that $n = 4$ and $m = 2$. If $v_i = [x, a, b, x]^T$, where a and b are the designer-specified components and x is the unspecified component, it is clear that $v_i^d = [a, b]^T$. In this case, to guarantee $D v_i = v_i^d$ [see Eq. (16)], the matrix D becomes

$$D = \begin{bmatrix} 0 & 1 & 0 & 0 \\ 0 & 0 & 1 & 0 \end{bmatrix}$$

Also note that, because λ_i is an eigenvalue of A_c, from Eq. (16), one has

$$K C v_i = u_i \tag{17}$$

Finally, letting

$$V = [v_1, \ldots, v_i, \ldots, v_r] \tag{18}$$

$$U = [u_1, \ldots, u_i, \ldots, u_r] \tag{19}$$

we obtain

$$K = U(CV)^{-1} \tag{20}$$

In the calculations to follow, Eq. (20) is used to compute K.

To proceed further, we must evaluate the Z matrix in Eq. (15). Assume that n_r and n_c are the number of real eigenvalues and half of the complex eigenvalues of A_c, respectively. The Λ and T matrices in Eqs. (7) and (11) can be partitioned as follows:

$$\Lambda \equiv \begin{bmatrix} \Lambda_A & 0 \\ 0 & \Lambda_D \end{bmatrix}; \qquad T \equiv \begin{bmatrix} T_A & T_B \\ T_C & T_D \end{bmatrix} \tag{21}$$

where

$$\Lambda_A = \mathrm{diag}\left(\Lambda_{A_1}, \ldots, \Lambda_{A_{n_c}}\right)$$
$$\Lambda_D = \mathrm{diag}\left(\Lambda_{D_1}, \ldots, \Lambda_{D_{n_r}}\right) \tag{22}$$

$$\Lambda_{A_i} = \begin{bmatrix} \mathrm{Re}_i & \mathrm{Im}_i \\ -\mathrm{Im}_i & \mathrm{Re}_i \end{bmatrix}, \qquad i = 1, \ldots, n_c \tag{23}$$

$$\Lambda_{D_k} = [\lambda_k], \qquad k = 1, \ldots, n_r \tag{24}$$

Here Re and Im are real and imaginary parts of the generic complex eigenvalue; moreover, Λ_A, $T_A \in R^{2n_c \times 2n_c}$, $T_B \in R^{2n_c \times n_r}$, $T_C \in R^{n_r \times 2n_c}$, and Λ_D, $T_D \in R^{n_r \times n_r}$. With this choice, the modal matrix M is real valued and its columns are the real and imaginary parts of the eigenvectors of A_c (if the corresponding eigenvalues are complex) or just the real eigenvectors (otherwise).

From Eqs. (21–24), Eq. (12) becomes

$$\Phi \equiv \begin{bmatrix} \Phi_A & 0 \\ 0 & \Phi_D \end{bmatrix} \tag{25}$$

where

$$\Phi_A = \mathrm{diag}\left(\Phi_{A_1}, \ldots, \Phi_{A_{n_c}}\right)$$
$$\Phi_D = \mathrm{diag}\left(\Phi_{D_1}, \ldots, \Phi_{D_{n_r}}\right) \tag{26}$$

$$\Phi_{A_i} = \begin{bmatrix} \exp(\mathrm{Re}_i t)\cos(\mathrm{Im}_i t) & \exp(\mathrm{Re}_i t)\sin(\mathrm{Im}_i t) \\ -\exp(\mathrm{Re}_i t)\sin(\mathrm{Im}_i t) & \exp(\mathrm{Re}_i t)\cos(\mathrm{Im}_i t) \end{bmatrix}$$
$$i = 1, \ldots, n_c \tag{27}$$

$$\Phi_{D_k} = [\exp(\lambda_k t)], \qquad k = 1, \ldots, n_r \tag{28}$$

Finally, from Eq. (15) the following expression of Z is obtained:

$$Z = \begin{bmatrix} \int_0^\infty \left(\Phi_A^T T_A \Phi_A\right) \mathrm{d}t & \int_0^\infty \left(\Phi_A^T T_B \Phi_D\right) \mathrm{d}t \\ \int_0^\infty (\Phi_D T_C \Phi_A) \, \mathrm{d}t & \int_0^\infty (\Phi_D T_D \Phi_D) \, \mathrm{d}t \end{bmatrix} \tag{29}$$

Observe that, in deriving Eq. (29), we used the fact that $\Phi_D^T = \Phi_D$.

To compute PI, the integrals in Eq. (29) are needed. The key point is that it is possible to calculate the above integrations in closed form. Details are given in the Appendix.

Problem Statement and Solution

The problem can be stated as follows: Try to minimize the PI given in Eq. (13) while putting some (suitable) constraints on the eigenvalues and eigenvectors of A_c (i.e., on the controlled system). In doing so, it is convenient to work with complex eigenvalues in polar form. In fact, calling $\omega_i \exp(\pm j\theta_i)$ the generic pair of complex eigenvalues and λ_i the generic real eigenvalue, flying-quality requirements are easily taken into account as follows[2]:

$$\omega_i^{(\min)} \le \omega_i \le \omega_i^{(\max)}, \qquad \theta_i^{(\min)} \le \theta_i \le \theta_i^{(\max)} \tag{30}$$

$$\lambda_i^{(\min)} \le \lambda_i \le \lambda_i^{(\max)} \tag{31}$$

where the superscripts min and max denote minimum and maximum values attained by the indicated variables. Now, define η, the vector containing the eigenvalues of A_c, and w^d, the vector containing the components of the desired eigenvectors of A_c. Observe that, from Eqs. (16–20), the K matrix is a function of η and w^d, and so is the PI. Hence, the problem consists of minimizing Eq. (13), while taking into account constraints (30) and (31) on the eigenvalues and the inequality

$$v_i^{d(\min)} \le v_i^d \le v_i^{d(\max)} \tag{32}$$

on the eigenvector of A_c. In the following, the index i in Eqs. (30–32) is limited to those components of η and w^d that we want to change with respect to the initial configuration. Note that the maximum deflection of the control surfaces is automatically taken into account with a suitable choice of the R matrix in Eq. (6). As a first choice of R, one could employ, for example, Bryson's rule.[18]

The numerical algorithm for the determination of the PI can now be summarized as follows: Assume that the values of η, w^d, and J at the kth iteration are known. At the next $(k+1)$ iteration, η and w^d are changed [making use of first-order gradient information on the objective function and constraints (30–32)], so as to determine a search direction that reduces $J(\eta, w^d)$ while maintaining a feasible design. Moreover, the current value of K is evaluated from Eqs. (16–20). Next, J is updated using Eqs. (13), (14), and (29) and the results in the Appendix. This process is repeated until the difference between consecutive values of the objective function is small enough.

To improve the convergence speed of the algorithm, a closed-form expression of the first-order gradient of PI may be used. The formulas related to this problem have been developed but are omitted here because of space limitations. However, the approach is similar to that used by the author in a previous paper.[19]

To avoid a great number of parameters in the minimization process, it is useful (albeit not necessary) to fix a priori the components of the desired eigenvectors. In particular, the eigenvector components can be chosen so as to decouple, at least partially, some natural modes of the controlled aircraft. In this way, only the eigenvalue positions in the complex plane are optimized.

Numerical Examples

We compare our technique with the results obtained by Andry et al.[5] We consider the lateral dynamics of the L-1011 aircraft at cruise flight condition. The A, B, and C matrices are given by

$$A = \begin{bmatrix} -20 & 0 & 0 & 0 & 0 & 0 & 0 \\ 0 & -25 & 0 & 0 & 0 & 0 & 0 \\ 0 & 0 & 0 & 0 & 1 & 0 & 0 \\ -0.744 & -0.032 & 0 & -0.154 & -0.0042 & 1.54 & 0 \\ 0.337 & -1.12 & 0 & 0.249 & -1.0 & -5.2 & 0 \\ 0.02 & 0 & 0.0386 & -0.996 & -0.000295 & -0.117 & 0 \\ 0 & 0 & 0 & 0.5 & 0 & 0 & -0.5 \end{bmatrix} \tag{33}$$

$$B^T = \begin{bmatrix} 20 & 0 & 0 & 0 & 0 \\ 0 & 25 & 0 & 0 & 0 \end{bmatrix} \tag{34}$$

$$C = \begin{bmatrix} 0 & 0 & 0 & 1 & 0 & 0 & -1 \\ 0 & 0 & 0 & 0 & 1 & 0 & 0 \\ 0 & 0 & 0 & 0 & 0 & 1 & 0 \\ 0 & 0 & 1 & 0 & 0 & 0 & 0 \end{bmatrix} \tag{35}$$

and the state vector x is defined as

$$x^T = [\delta_r, \delta_a, \varphi, r, p, \beta, x_{\mathrm{wo}}] \tag{36}$$

where δ_r is the rudder deflection, δ_a is the aileron deflection, φ is the bank angle, r is the yaw rate, p is the roll rate, β is the sideslip angle, and x_{wo} is the washout filter state. The system inputs are the rudder command δ_{rc} and the aileron command δ_{ac}, and the system outputs are

$$y^T = [r_{\mathrm{wo}}, p, \beta, \varphi] \tag{37}$$

where r_{wo} is the washed-out yaw rate. The open-loop eigenvalues are

$$\lambda_{\mathrm{OL}}^T = [-20.0, -25.0, -0.0882 \pm j1.2695, \\ -0.0091, -1.0855, -0.5] \tag{38}$$

In Eq. (38) the rudder and aileron modes, the dutch-roll mode, the spiral mode, the roll mode, and the washout filter mode are recognized.

In this example, we want to increase the dutch-roll damping ratio and obtain a couple of complex conjugate poles to describe the roll mode. At the same time, we want to decouple the dutch-roll from the roll mode and, to this end, we choose to null the entries of the dutch roll eigenvector corresponding to φ and p states and the entries of the roll eigenvector corresponding to β and x_{wo} states. We use the following eigenvalue constraints[2]:

$$1 \le \omega_{\mathrm{DR}} \le 3, \qquad 0.2 \le \zeta_{\mathrm{DR}} \le 1 \qquad \text{dutch-roll mode} \tag{39}$$

$$1 \le \omega_R \le 3, \qquad 0.2 \le \zeta_R \le 1 \qquad \text{roll mode} \tag{40}$$

where ω and ζ are the eigenvalue natural frequency and damping ratio. Note that the relationship between θ [given by Eq. (30)] and ζ in Eqs. (39) and (40) is $\theta = \arcsin \zeta + \pi/2$; this means that the constraint $0.2 \le \zeta \le 1$ is equivalent to $1.7721 \le \theta \le 3.1415$. Moreover, we set

$$Q = \mathrm{diag}(0, 0, 1, 1, 1, 1, 1) \tag{41}$$

and we employ two different values for R, namely,

$$R = \mathrm{diag}(0.3, 0.3), \qquad \text{case 1} \tag{42}$$

$$R = \mathrm{diag}(10, 10), \qquad \text{case 2} \tag{43}$$

As a further example, we compare the results obtained in the above two cases with a third case in which we force the roll and spiral poles to be real valued. For this example (case 3), we use the

Table 1 Comparison between closed-loop eigenvalues

Case	Rudder mode	Aileron mode	Dutch-roll mode	Roll + spiral mode	Washout filter mode
Andry et al.[5]	−17.05	−22.01	$-1.50 \pm j\,1.50$ $\zeta = 0.7083, \omega = 2.12$	$-2.0012 \pm j0.9995$ $\zeta = 0.8946, \omega = 2.24$	−0.6989
1	−18.35	−23.09	$-0.8744 \pm j\,1.5468$ $\zeta = 0.4921, \omega = 1.78$	$-1.4740 \pm j\,0.0051$ $\zeta = 0.9999, \omega = 1.47$	−0.6305
2	−18.64	−24.71	$-0.7542 \pm j\,1.5747$ $\zeta = 0.4320, \omega = 1.75$	$-0.6573 \pm j\,0.7536$ $\zeta = 0.6574, \omega = 1.00$	−0.6016
3	−16.48	−22.95	$-1.3044 \pm j\,0.0170$ $\zeta = 0.9999, \omega = 1.30$	−3.00 −0.001	−1.7215

Table 2 Comparison between closed-loop eigenvectors

	Andry et al.[5]		Case 1		Case 2		Case 3	
	Dutch roll	Roll	Dutch roll	Roll	Dutch roll	Roll	Dutch roll	Roll
δ_r	$0.7277 \pm j0.2285$	$-0.0312 \pm j0.0245$	$0.0979 \pm j0.5014$	$0.0334 \pm j0.0460$	$0.4515 \pm j0.0395$	$0.0299 \pm j0.0143$	$-0.7107 \pm j0.2647i$	0.0696
δ_a	$0.2861 \pm j0.4863$	$0.5585 \pm j0.5013$	$0.7701 \pm j0.1537$	$-0.1842 \pm j0.2496$	$0.4498 \pm j0.6839$	$0.0646 \pm j0.4599$	$0.5239 \pm j0.2074$	−0.8531
φ	$0.0004 \pm j0.0001$	$0.1130 \pm j0.2443$	$0 \pm j0$	$0.3099 \pm j0.4331$	$0 \pm j0$	$0.2470 \pm j0.5746$	$-0.0002 \pm j0.0001$	0.1635
r	$0.2017 \pm j0.1912$	$0.0007 \pm j0.0018$	$-0.1037 \pm j0.2752$	$0.0128 \pm j0.0179$	$0.2243 \pm j0.1926$	$0.0103 \pm j0.0220$	$-0.2172 \pm j0.0807$	0.0079
p	$-0.0009 \pm j0.0002$	$0.0180 \pm j0.6020$	$0.0001 \pm j0.0003$	$-0.4590 \pm j0.6369$	$-0.0002 \pm j0.0002$	$-0.5954 \pm j0.1916$	$0.0002 + j0.0001$	−0.4905
β	$-0.0048 \pm j0.1290$	$-0.0031 \pm j0.0028$	$-0.1646 \pm j0.0125$	$0 \pm j0$	$-0.0569 \pm j0.1592$	$0 \pm j0$	$-0.1693 \pm j0.0657$	0
x_{wo}	$0.0130 \pm j0.0761$	$-0.0004 \pm j0.0003$	$0.0917 \pm j0.0113$	$-0.0065 \pm j0.0092$	$0.0484 \pm j0.0790$	$0.0126 \pm j0.0095$	$0.1339 \pm j0.0530$	−0.0016

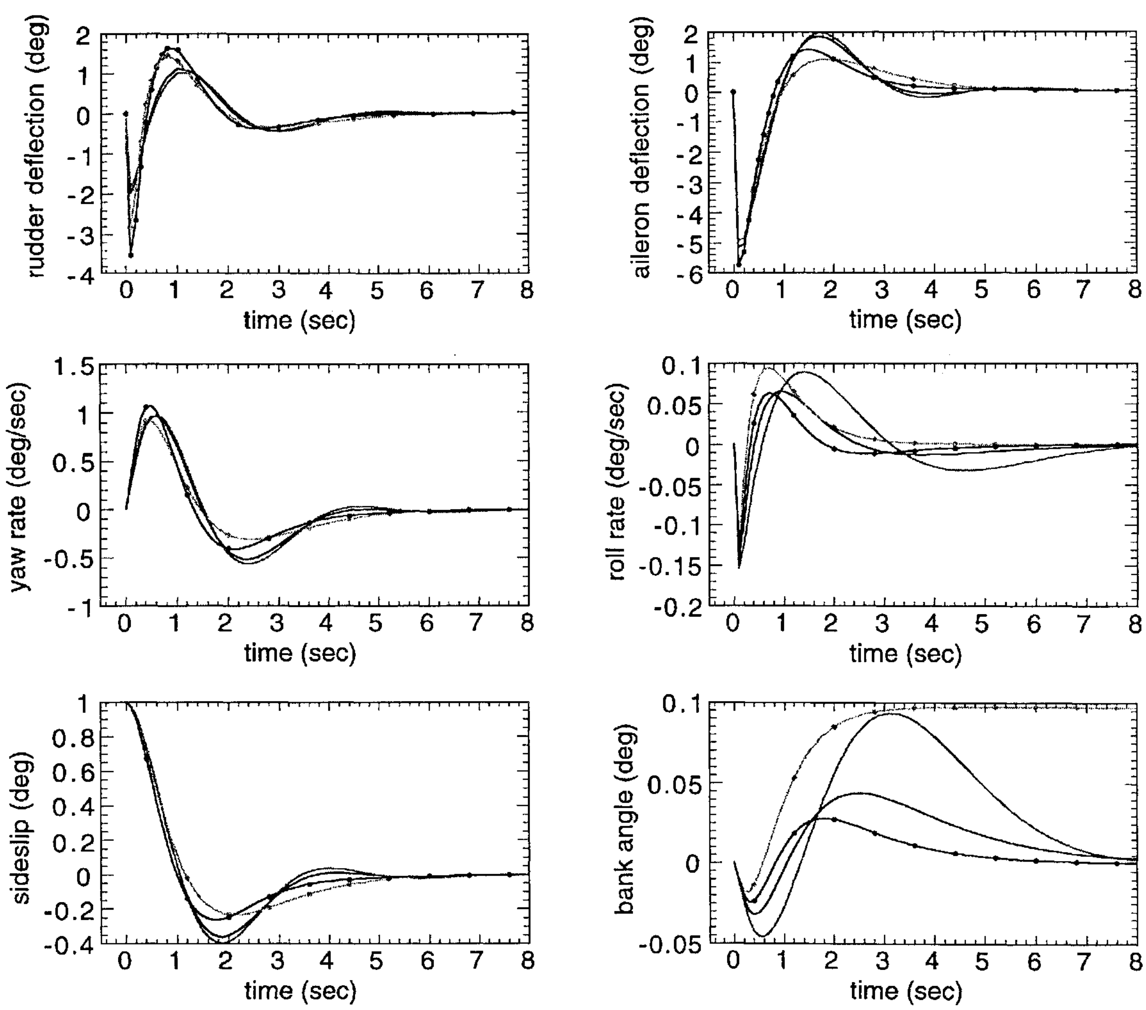

Fig. 1 Comparison between time histories of closed-loop systems relative to an initial sideslip angle of 1 deg: ——, case 1; · · · · ·, case 2; ♦, case 3; and •, Andry et al.[5]

same constraints on the eigenvectors as before and the following eigenvalue constraints:

$$1 \le \omega_{DR} \le 3, \qquad 0.2 \le \zeta_{DR} \le 1 \qquad \text{dutch-roll mode} \quad (44)$$

$$-3 \le \lambda_R \le -0.714 \qquad \text{roll mode} \quad (45)$$

$$-0.001 \le \lambda_S \le 0 \qquad \text{spiral mode} \quad (46)$$

along with a Q matrix given by Eq. (41) and

$$R = \text{diag}(0.3, 0.3) \quad (47)$$

In Eq. (45), the value −0.714 for the upper constraint of the roll mode was selected so as to meet level 1 of flying-quality requirements.[2] Our results are summarized in Tables 1–3.

Note that the states have not been scaled with respect to their maximum value so as to get adimensional eigenvectors. This would ease the identification of the dominant modes associated with a particular eigenvalue.[8] Dimensional equations have been used, instead, for a simple comparison with the results of Andry et al.[5]

A few comments are in order. First, in all cases the dutch-roll mode is well decoupled from the roll mode, as is apparent from Table 2. Second, comparing case 1 and case 2, one appreciates the effect of input weighting imposed by the matrix R. In particular, from Table 3 it is seen that all entries of the gain matrix K in case 2 are smaller (in absolute value) than the corresponding entries of case 1. In terms of eigenvalue location, cases 1 and 2 differ, in practice, only in the position of the complex roll poles. In particular, the roll poles are nearly real valued ($\zeta \approx 1$) in case 1, but in case 2, a constraint is imposed on the maximum value of the roll-mode natural frequency. Also, in both cases, the roll poles are on the boundary of the admissible region defined by Eq. (40).

Table 3 Comparison between gain matrices

Case	Gain matrix, K
Andry et al.[5]	$\begin{bmatrix} -3.350 & 0.159 & 4.880 & 0.379 \\ -1.420 & -2.380 & 6.360 & -3.800 \end{bmatrix}$
1	$\begin{bmatrix} -1.973 & 0.158 & 2.676 & 0.257 \\ -1.013 & -1.556 & 5.660 & -1.682 \end{bmatrix}$
2	$\begin{bmatrix} -1.676 & 0.120 & 2.398 & 0.154 \\ -0.924 & -0.253 & 5.566 & -0.816 \end{bmatrix}$
3	$\begin{bmatrix} -3.855 & 0.049 & 4.073 & 0.008 \\ -1.727 & -1.567 & 6.514 & -0.009 \end{bmatrix}$

Table 4 Comparison between peak values (in degrees) of rudder and aileron, relative to an initial sideslip angle of 1 deg

	Andry et al.[5]	Case 1	Case 2	Case 3
δ_r	−3.52	−1.98	−1.80	−2.82
δ_a	−5.74	−5.15	−4.92	−5.72

Table 5 Comparison between peak values (in degrees) of rudder and aileron, relative to an initial bank angle of 1 deg

	Andry et al.[5]	Case 1	Case 2	Case 3
δ_r	−0.30	−0.21	−0.13	−0.027
δ_a	3.12	1.43	0.76	−0.092

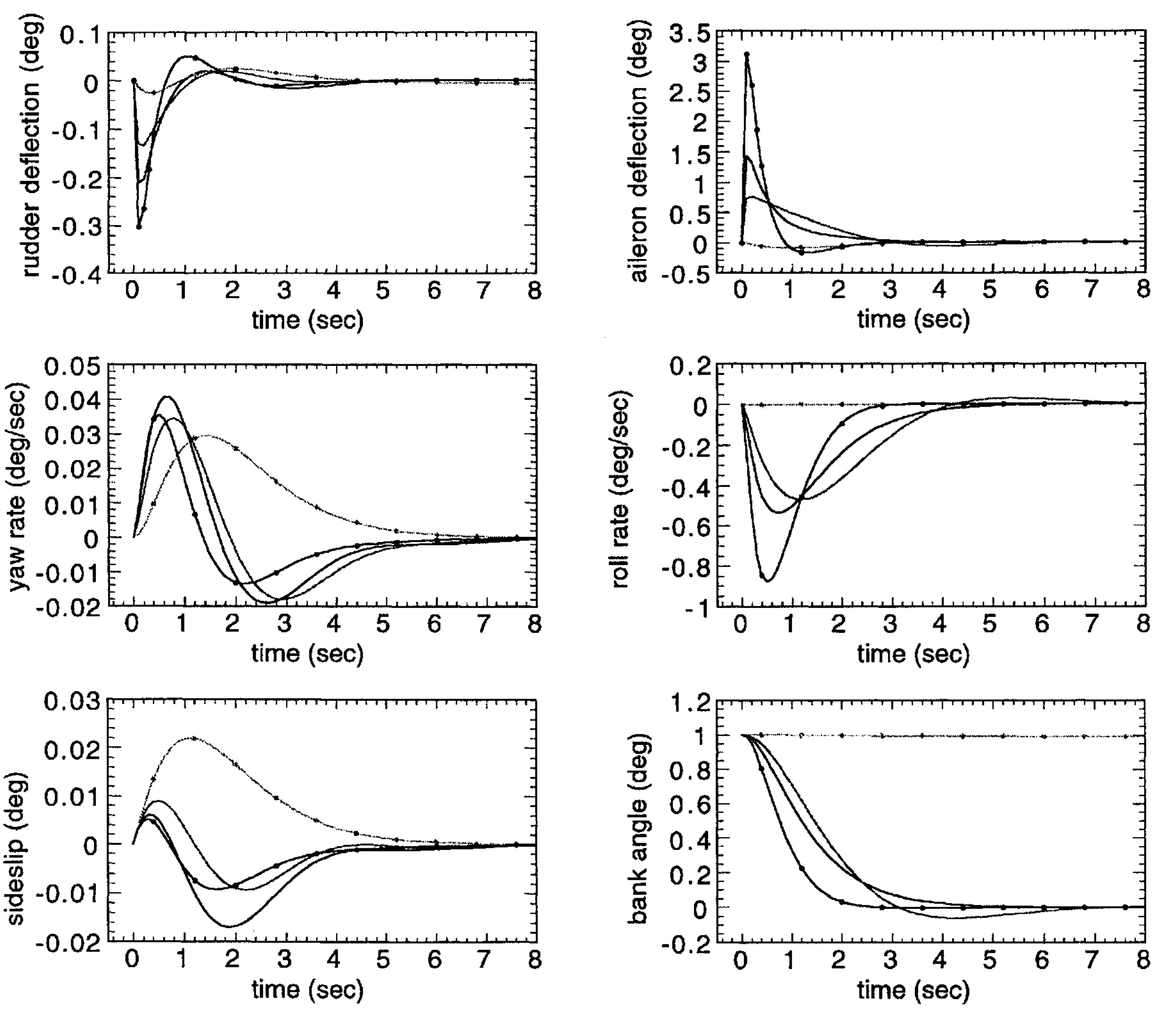

Fig. 2 Comparison between time histories of closed-loop systems relative to an initial bank angle of 1 deg: ——, case 1; · · · · ·, case 2; ♦, case 3; and •, Andry et al.[5]

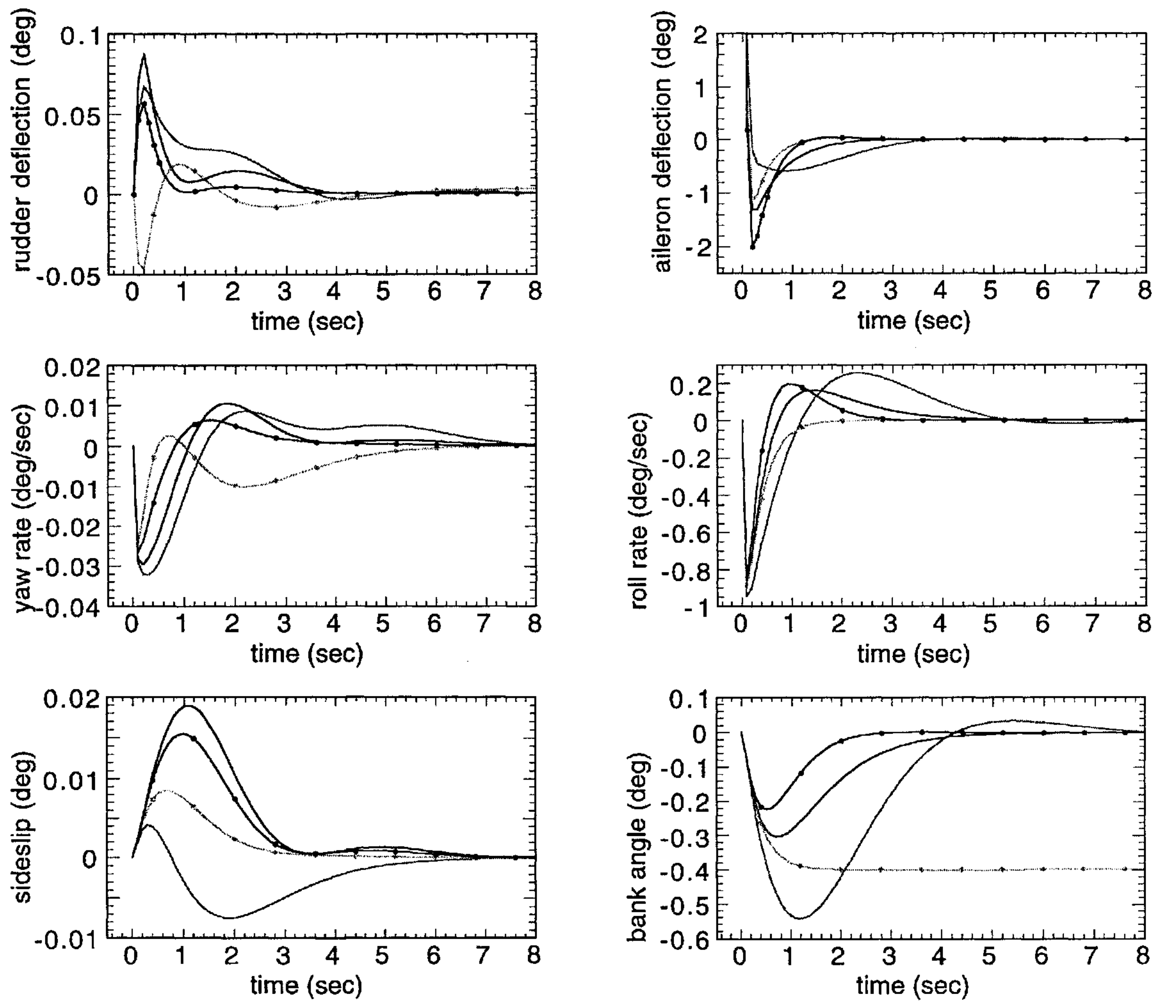

Fig. 3 Comparison between time histories of closed-loop systems relative to an aileron impulse of 1 deg: ——, case 1; · · · · ·, case 2; ♦, case 3; and •, Andry et al.[5]

The closed-loop transient responses for the three cases are compared to those given by Andry et al.[5] in Figs. 1–3. In Figs. 1 and 2 the time histories correspond to an initial sideslip angle (Fig. 1) or bank angle (Fig. 2) of 1 deg, while all other initial conditions are zero. The substantial reduction of the peaks in the rudder and aileron deflections with respect to Andry et al.[5] is apparent in all cases. A quantitative information about the peak values is given in Tables 4 and 5. The greater peak reduction is obtained in case 2, as is expected in view of the preceding discussion on the K entries. Also, the tradeoff between the will to obtain fast time responses and the need to limit the control demand can clearly be appreciated from Figs. 1 and 2, paralleling cases 1 and 2. In particular, observe that, in case 1, the reduction in input demand, as compared with that of Andry et al.,[5] has been obtained without a substantial degradation in output responses.

We stress the fact that, as expected, all variables in Figs. 1 and 2 go to zero as time increases. This is true also for roll response of case 3, although this is not apparent. This is attributable to a scale problem; in fact in cases 1 and 2, the bank angle returns to zero within a few seconds, whereas, in case 3, it takes 3 to 4 times the spiral mode (approximately 4000 s), as is seen in Table 1, where it is found that the spiral pole value is −0.001.

Case 3 differs drastically from the others because of the presence of a pole near the origin, the spiral pole. This example is interesting because the final eigenvalue/eigenvector configuration is similar to an ideal open-loop aircraft model wherein a pilot must command the aircraft with an impulsive input on the aileron surface to obtain a finite value of bank angle with no excitation of the dutch-roll mode. This fact is apparent from Fig. 3 and also from the analysis of the transfer function between the aileron input and the bank angle for the closed-loop system of case 3. This function is found to be

$$\frac{\varphi}{\delta_{ac}} = \frac{-28(s+16.47)(s+1.70)}{(s+22.95)(s+16.48)(s+1.72)(s+0.001)(s+3)} \tag{48}$$

from which it is clear that we have no dutch roll at all. Furthermore, the rudder pole and the washout filter pole are almost cancelled out by the corresponding zeros in the transfer function.

Finally, note that the algorithm tends to eliminate some right half plane zeros. For instance, in the open-loop case, one has

$$\frac{\varphi}{\delta_{rc}} = \frac{6.74(s+2.88)(s-3.47)}{(s^2+0.177s+1.62)(s+1.09)(s+0.009)(s+20)} \tag{49}$$

whereas, for case 3, the right half plane zero of Eq. (49) is no longer present; indeed the corresponding transfer function is

$$\frac{\varphi}{\delta_{rc}} = \frac{6.74(s+2.35)(s+19.97)(s^2+2.6s+1.694)}{(s+22.95)(s+16.48)(s+1.72)(s+0.001)(s+3)} \tag{50}$$

Conclusions

A mixed LQ/eigenstructure assignment approach has been proposed to design aircraft stability augmentation systems. The procedure employs a standard LQ performance criterion and a numerical optimization process to obtain an optimum static output-feedback controller. In our technique, some components of the desired eigenvectors and the eigenvalue location are allowed to vary within prescribed boundaries and their values are optimized. In this way the following tasks are achieved: 1) the eigenvalue position is constrained according to flying-quality requirements; 2) some modes of the response of the closed-loop system are decoupled (at least partially); and 3) maximum deflection and rate of deflection of the input commands are optimized by choosing a proper structure of weighting matrices R and Q. Keys to this approach are a relation between gain matrix K and eigenstructure of the closed-loop system; a closed-form evaluation of the PI as a function of K. The latter result produces a fast numerical algorithm.

As a final remark, observe that in the original Harvey–Stein approach[11] some closed-loop eigenvalues were specified, whereas others (usually taken to be the actuator poles) were allowed to move to some arbitrary position in the complex plane. However, unacceptably large closed-loop actuator bandwidth sometimes resulted if the actual closed-loop poles were forced to get close to their specified values. It is apparent that our approach, which places poles only in some specified regions, mitigates the described drawback.

The proposed procedure is simple to handle and can be effectively employed to get quick solutions for the designer. Examples indicate good improvements with respect to a classic eigenstructure approach.

Appendix: Computation of the Matrix Z

We compute the matrix Z in Eq. (29). To start, denote $A = \{a(i,k)\}$ a matrix with entries $a(i,k)$. Also define $\boldsymbol{w}_r$ and $\boldsymbol{w}_i$ as the vectors containing real and imaginary-positive parts of the complex poles of A_c. Note that $\boldsymbol{w}_r \in R^{n_r}$ and $\boldsymbol{w}_i \in R^{n_c}$. Finally, let

$$\mu = \begin{cases} (i+1)/2 & \text{if} \quad i = \text{odd} \\ i/2 & \text{if} \quad i = \text{even} \end{cases} \tag{A1}$$

$$\nu = \begin{cases} (k+1)/2 & \text{if} \quad k = \text{odd} \\ k/2 & \text{if} \quad k = \text{even} \end{cases} \tag{A2}$$

$$\beta_p = w_i(\nu) + w_i(\mu) \tag{A3}$$

$$\beta_m = w_i(\nu) - w_i(\mu) \tag{A4}$$

$$\alpha = w_r(\nu) + w_r(\mu) \tag{A5}$$

$$T_A = \{t_A(i,k)\}, \qquad T_B = \{t_B(i,k)\}$$
$$T_C = \{t_C(i,k)\}, \qquad T_D = \{t_D(i,k)\} \tag{A6}$$

$$\Lambda_D = \{\lambda_D(i,k)\} \tag{A7}$$

With the preceding definitions, we now compute the four integrals appearing in Eq. (29).

1) Evaluation of

$$\{\chi(i,k)\} \equiv \int_0^\infty \left(\Phi_A^T T_A \Phi_A\right) \mathrm{d}t$$

case a) i = odd and k = odd

$$\{\chi(i,k)\} = \frac{1}{2}\left\{ -\left(\frac{\alpha}{\alpha^2+\beta_p^2} + \frac{\alpha}{\alpha^2+\beta_m^2}\right) t_A(i,k) + \left(\frac{-\beta_p}{\alpha^2+\beta_p^2} + \frac{\beta_m}{\alpha^2+\beta_m^2}\right) t_A(i+1,k) + \left[-\left(\frac{\beta_p}{\alpha^2+\beta_p^2} + \frac{\beta_m}{\alpha^2+\beta_m^2}\right) t_A(i,k+1)\right] + \left(\frac{\alpha}{\alpha^2+\beta_p^2} - \frac{\alpha}{\alpha^2+\beta_m^2}\right) t_A(i+1,k+1)\right\} \tag{A8}$$

case b) i = even and k = odd

$$\{\chi(i,k)\} = \frac{1}{2}\left\{ -\left(\frac{\alpha}{\alpha^2+\beta_p^2} + \frac{\alpha}{\alpha^2+\beta_m^2}\right) t_A(i,k) + \left(\frac{\beta_p}{\alpha^2+\beta_p^2} + \frac{-\beta_m}{\alpha^2+\beta_m^2}\right) t_A(i-1,k) + \left[-\left(\frac{\beta_p}{\alpha^2+\beta_p^2} + \frac{\beta_m}{\alpha^2+\beta_m^2}\right) t_A(i,k+1)\right] + \left(\frac{-\alpha}{\alpha^2+\beta_p^2} + \frac{\alpha}{\alpha^2+\beta_m^2}\right) t_A(i-1,k+1)\right\} \tag{A9}$$

case c) i = odd and k = even

$$\{\chi(i,k)\} = \frac{1}{2}\left[-\left(\frac{\alpha}{\alpha^2+\beta_p^2} + \frac{\alpha}{\alpha^2+\beta_m^2}\right) t_A(i,k) + \left(\frac{-\beta_p}{\alpha^2+\beta_p^2} + \frac{\beta_m}{\alpha^2+\beta_m^2}\right) t_A(i+1,k) + \left(\frac{\beta_p}{\alpha^2+\beta_p^2} + \frac{\beta_m}{\alpha^2+\beta_m^2}\right) t_A(i,k-1) + \left(\frac{-\alpha}{\alpha^2+\beta_p^2} + \frac{\alpha}{\alpha^2+\beta_m^2}\right) t_A(i+1,k-1)\right] \tag{A10}$$

case d) i = odd and k = even

$$\{\chi(i,k)\} = \frac{1}{2}\left[-\left(\frac{\alpha}{\alpha^2+\beta_p^2} + \frac{\alpha}{\alpha^2+\beta_m^2}\right) t_A(i,k) + \left(\frac{\beta_p}{\alpha^2+\beta_p^2} - \frac{\beta_m}{\alpha^2+\beta_m^2}\right) t_A(i-1,k) + \left(\frac{\beta_p}{\alpha^2+\beta_p^2} + \frac{\beta_m}{\alpha^2+\beta_m^2}\right) t_A(i,k-1) + \left(\frac{\alpha}{\alpha^2+\beta_p^2} - \frac{\alpha}{\alpha^2+\beta_m^2}\right) t_A(i-1,k-1)\right] \tag{A11}$$

2) Evaluation of

$$\{\chi(i,k)\} \equiv \int_0^\infty \left(\Phi_A^T T_B \Phi_D\right) \mathrm{d}t$$

case a) i = odd

$$\{\chi(i,k)\} = \left\{ -\frac{[\lambda_D(k,k) + w_r(\mu)] t_B(i,k) + w_i(\mu) t_B(i+1,k)}{[\lambda_D(k,k) + w_r(\mu)]^2 + [w_i(\mu)]^2} \right\} \tag{A12}$$

case b) i = even

$$\{\chi(i,k)\} = \left\{ \frac{-[\lambda_D(k,k) + w_r(\mu)] t_B(i,k) + w_i(\mu) t_B(i-1,k)}{[\lambda_D(k,k) + w_r(\mu)]^2 + [w_i(\mu)]^2} \right\} \tag{A13}$$

3) Evaluation of

$$\{\chi(i,k)\} \equiv \int_0^\infty \left(\Phi_D T_C \Phi_A\right) \mathrm{d}t$$

case a) k = odd

$$\{\chi(i,k)\} = \left\{ -\frac{[\lambda_D(i,i) + w_r(\nu)] t_C(i,k) + w_i(\nu) t_C(i,k+1)}{[\lambda_D(i,i) + w_r(\nu)]^2 + [w_i(\nu)]^2} \right\} \tag{A14}$$

case b) k = even

$$\{\chi(i,k)\} = \left\{ \frac{-[\lambda_D(i,i) + w_r(\nu)] t_C(i,k) + w_i(\nu) t_C(i,k-1)}{[\lambda_D(i,i) + w_r(\nu)]^2 + [w_i(\nu)]^2} \right\} \tag{A15}$$

4) Evaluation of

$$\{\chi(i,k)\} \equiv \int_0^\infty \left(\Phi_D T_D \Phi_D\right) \mathrm{d}t$$

Putting

$$\int_0^\infty (\Phi_D T_D \Phi_D)\,\mathrm{d}t = \{\chi(i,k)\}$$

we have

$$\{\chi(i,k)\} = \left\{-\frac{t_D(i,k)}{\lambda_D(i,i)+\lambda_D(k,k)}\right\} \tag{A16}$$

To summarize, Eqs. (A1–A16) allow us to calculate the Z matrix given by Eq. (29). Bearing in mind Eq. (13), the PI is immediately evaluated. Note that by virtue of the results of this Appendix, the PI is obtained in closed form, thus providing an efficient numerical algorithm.

References

[1]McRuer, D., and Graham, D., "Eighty Years of Flight Control: Triumphs and Pitfalls of the Systems Approach," *Journal of Guidance and Control*, Vol. 4, No. 4, 1981, pp. 353–362.

[2]Anon., "Flying Qualities of Piloted Airplanes," MIL-SPEC MIL-F-8785 C, Nov. 1980.

[3]Moore, B. C., "On the Flexibility Offered by State Feedback in Multivariable Systems Beyond Closed Loop Eigenvalue Assignment," *IEEE Transactions on Automatic Control*, Vol. AC-21, No. 5, 1976, pp. 689–692.

[4]Srinathkumar, S., "Eigenvalue/Eigenvector Assignment Using Output Feedback," *IEEE Transactions on Automatic Control*, Vol. AC-23, No. 1, 1978, pp. 79–81.

[5]Andry, A. N., Jr., Shapiro, E. J., and Chung, J. C., "Eigenstructure Assignment for Linear Systems," *IEEE Transactions on Aerospace and Electronic Systems*, Vol. AES-19, No. 5, 1983, pp. 711–729.

[6]Sobel, K. M., and Shapiro, E. Y., "Application of Eigenstructure Assignment to Flight Control Design: Some Extensions," *Journal of Guidance, Control, and Dynamics*, Vol. 10, No. 1, 1987, pp. 73–81.

[7]Mudge, S. K., and Patton, R. J., "Analysis of the Technique of Robust Eigenstructure Assignment with Application to Aircraft Control," *IEE Proceedings*, Vol. 135, Pt. D, No. 4, 1988, pp. 275–281.

[8]Garrard, W. L., Low, E., and Proudy, S., "Design of Attitude and Rate Command Systems for Helicopters Using Eigenstructure Assignment," *Journal of Guidance, Control, and Dynamics*, Vol. 12, No. 6, 1989, pp. 783–791.

[9]Innocenti, M., and Stanziola, C., "Performance-Robustness Trade Off of Eigenstructure Assignment Applied to Rotorcraft," *Aeronautical Journal*, Vol. 94, No. 934, 1990, pp. 124–131.

[10]Low, E., and Garrard, W. L., "Design of Flight Control Systems to Meet Rotorcraft Handling Qualities Specifications," *Journal of Guidance, Control, and Dynamics*, Vol. 16, No. 1, 1993, pp. 69–78.

[11]Harvey, C. A., and Stein, G., "Quadratic Weights for Asymptotic Regulator Properties," *IEEE Transactions on Automatic Control*, Vol. AC-23, No. 3, 1978, pp. 378–387.

[12]Huang, J. C., and Lee, T. T., "On Optimal Pole Assignment in a Specified Region," *International Journal of Control*, Vol. 40, No. 1, 1984, pp. 65–79.

[13]Kim, S. B., and Furuta, K., "Regulator Design with Poles in a Specified Region," *International Journal of Control*, Vol. 47, No. 1, 1988, pp. 143–160.

[14]Kawasaki, N., and Shimemura, E., "Pole Placement in a Specified Region Based on a Linear Quadratic Regulator," *International Journal of Control*, Vol. 48, No. 2, 1988, pp. 225–240.

[15]Haddad, W. M., and Bernstein, D. S., "Controller Design with Regional Pole Constraints," *IEEE Transactions on Automatic Control*, Vol. AC-37, No. 1, 1992, pp. 54–69.

[16]Slater, G. L., and Zhang, Q., "Controller Design by Eigenspace Assignment," *Mechanics and Control of Large Flexible Structures*, Vol. 129, Progress in Astronautics and Aeronautics, AIAA, Washington, DC, 1990, pp. 435–462.

[17]Levine, W. S., and Athans, M., "On the Determination of the Optimal Constant Output-Feedback Gains for Linear Multivariable Systems," *IEEE Transactions on Automatic Control*, Vol. AC-15, No. 2, 1970, pp. 44–48.

[18]Bryson, A. E., Jr., and Ho, Y. C., *Applied Optimal Control*, Hemisphere, Washington, DC, 1975, pp. 148–149.

[19]Mengali, G., "Ride Quality Improvements by Means of Numerical Optimization Techniques," *Journal of Guidance, Control, and Dynamics*, Vol. 17, No. 5, 1994, pp. 1037–1041.